ORNL/TM-12401

ornl

OAK RIDGE NATIONAL LABORATORY

MARTIN MARIETTA

# Solubility Measurement of Uranium in Uranium-Contaminated Soils

S. Y. Lee
Mark Elless
Forrest Hoffman

Environmental Sciences Division
Publication No 4138



MANAGED BY
MARTIN MARIETTA ENERGY SYSTEMS INC.
FOR THE UNITED STATES
DEPARTMENT OF ENERGY

ORNL/TM-12401

902
11

# Solubility Measurement of Uranium in Uranium-Contaminated Soils

S. Y. Lee, Mark Elless, and Forrest Hoffman

Environmental Sciences Division
Publication No. 4138

Date Issued—August 1993

Prepared for
In Situ Remediation Integrated Program
Office of Technology Development

Prepared by the
Oak Ridge National Laboratory
Oak Ridge, Tennessee 37831

managed by
Martin Marietta Energy Systems, Inc.
for the
U.S. DEPARTMENT OF ENERGY
under contract DE-AC05-84OR21400

# TABLE OF CONTENTS

ACKNOWLEDGMENTS . . . . . v
ABSTRACT . . . . . vii
1. INTRODUCTION . . . . . 1
2. MATERIAL AND METHODS . . . . . 2
3. RESULTS AND DISCUSSION . . . . . 5
4. SUMMARY AND RECOMMENDATIONS . . . . . 19
5. LITERATURE CITED . . . . . 20
APPENDIX . . . . . 23

# ACKNOWLEDGMENTS

This soil equilibration experiment was supported by the supplemental funding of the In Situ Remediation Integrated Program. This program was coordinated by Mary E. Paterson, Battelle Pacific Northwest Laboratory and established by the DOE Office of Technology Development. Characterization section of the uranium contaminated soil in this report was supported by the Uranium Soil Integrated Demonstration Program coordinated by Kim Nuhfer, Fernald Environmental Restoration Management Corporation. The authors thank both coordinators for their support.

# ABSTRACT

A short-term equilibration study involving two uranium-contaminated soils at the Department of Energy's Fernald Environmental Management Program (FEMP) site was conducted as part of the In Situ Remediation Integrated Program. The goal of this study is to predict the behavior of uranium during on-site remediation of these soils. Geochemical modeling was performed on the aqueous species dissolved from these soils following the equilibration study to predict the on-site uranium leaching and transport processes. Results showed that the soluble levels of the major components (total uranium, calcium, magnesium, and carbonate) increased continually for the first four weeks. After the first four weeks, these components either reached a steady-state equilibrium (in those components having solubilities approaching that of the controlling solid phase for that component) or continued linearity throughout the study (in those components having low solubilities). Other major components, such as aluminum, potassium, and iron, reached a steady-state concentration within three days. Silica levels approximated the predicted solubility of quartz throughout the study. A much higher level of dissolved uranium was observed in the soil contaminated from spillage of uranium-laden solvents and process effluents than in the soil contaminated from settling of airborne uranium particles ejected from the nearby incinerator. The high levels observed for soluble calcium, magnesium, and bicarbonate are probably the result of magnesium and/or calcium carbonate minerals dissolving in these soils. The increase in the total uranium levels with increasing carbonate levels is due to the complexation of uranium with carbonate species. Geochemical modeling confirms that the uranyl-carbonate complexes are the most stable and dominant in these solutions. The implication of this work is that the use of carbonate minerals on these soils for erosion control and road construction activities contributes to the leaching of uranium from contaminated soil particles. Dissolved carbonates promote uranium solubility, forming highly mobile anionic species. Mobile uranium species are contaminating the groundwater underlying these soils. Therefore, the development of a site-specific remediation technology is urgently needed for the FEMP site.

# INTRODUCTION

Remediation of uranium-contaminated soils is currently considered a high priority within the U.S. Department of Energy (DOE) not only because these soils represent an environmental hazard, but also because these soils are a potential source of contamination of the underlying groundwater during natural leaching episodes. Therefore, the behavior of uranium under saturated conditions, particularly its complexation potential and mobility, must be understood for predicting the environmental impact these soils might have on the underlying groundwater quality.

The solubility of soil uranium depends upon the soil's physicochemical, mineralogical and micromorphological properties; the nature of the uranium association; and the mineralogical, morphological, and compositional characteristics of the uranium-bearing phases. In particular, uranium solubility is enhanced by the presence of dissolved carbonate species, especially if the uranium is in the hexavalent form (Bowie and Plant 1983; Francis et al. 1992). Uranyl-carbonate complexes are very strong and are often negatively charged. The negativity associated with these complexes allows them to be rather mobile in the soil environment and therefore represents a potential for groundwater contamination.

Uranium-contaminated soils from the Fernald Environmental Management Project (FEMP) site were selected for this study. Solubility of uranium-containing minerals and concentration of each uranium species in equilibrated soil solutions will be determined. The results of the FEMP study will be beneficial for the In Situ Remediation Integrated Program (ISRIP) and the Uranium Soil Integrated Demonstration (USID). This information is needed by ISRIP for its evaluation of FEMP as a potential in situ integrated demonstration site and by USID for chemical modeling and environmental assessment. As a part of the USID, two FEMP uranium-contaminated soils and several cores have been collected and partially characterized (Lee and Marsh 1992).

To ascertain the behavior of uranium solubility at the Fernald site, a short-term equilibration experiment using two uranium-contaminated FEMP soils was conducted. These two soils were selected because each represents a different mode of uranium contamination (airborne and spillage). This experimental approach has been commonly used to measure solubility of soil components and to identify soluble ionic and complex species of target components in soil solutions. The determination of solubility and chemical speciation will provide vital information for understanding contaminant behavior in these soils under natural conditions and during any in situ remediation demonstration.

Therefore, the objectives of this task are (1) to measure the solubility of the soil components in two uranium-contaminated soils, (2) to calculate the distribution of the dominant uranium species in the soil solution using a chemical speciation model, and (3) to compare the results of the soil equilibration approach with the known groundwater composition from this site. This study will submit results to (1) ISRIP, (2) the FEMP site remedial investigation team, and (3) the Characterization Task Group of the USID program.

# 2. MATERIAL AND METHODS

## 2.1 SOIL SAMPLING AND PRELIMINARY CHARACTERIZATION

FEMP personnel sampled and homogenized two FEMP soils for treatability tests by the USID Decontamination Task Group. One sample (B-16, Drum No. 6) was collected near the Plant 1 Storage Pad Area within the production area. The other sample (A-14, Drum No. 12) was collected near the Incinerator area located a few hundred yards east of the main plant area. The Characterization Task Group of the USID program took soil core samples from the same area and characterized their physicochemical and mineralogical properties (Lee and Marsh 1992). Each excavated area was ~ 25 x 20 ft, with an excavation depth of 6 to 8 inches (Kneff et al. 1992). Preliminary characterization of the samples was completed (Lee and Marsh 1992), but detailed characterization for treatability studies will be continued by the Characterization Task Group of the USID. Particle-size separations were performed on both FEMP soils to determine the uranium partitioning among the various size fractions. Particle size separations were performed by field moist sieving using 4- and 2-mm stainless steel sieves. Size fractions larger than 2 mm were designated as gravel. The <2-mm fractions were further separated into sand particles measuring 2 to 0.053 mm, silt particles ranging from 0.053 to 0.002 mm, and clay particles measuring <0.002 mm by wet sieving and centrifugation (Jackson 1975). These size-fractionated samples and the whole soils were then analyzed by neutron activation analysis for uranium quantification (Wade et al. 1992). Heavy liquid separations were also performed on the sand and silt fractions of both soils in an attempt to isolate a uranium-bearing fraction for later mineralogical analysis. Lithium metatungstate (LMT, $\rho$ = 3.0 g/cm$^3$) was the medium used in all density separations. Uranium quantification on all density fractions was determined by gamma spectroscopy (Larsen et al. 1992).

## 2.2 MINERALOGICAL CHARACTERIZATION

Scanning electron microscopy (SEM), using both secondary and backscattered electron imaging coupled with energy-dispersive X-ray analysis (EDX), was used for morphological analysis and particle-size/elemental distributions. A small amount of dry whole soil and size-fractionated samples of both soils was embedded in epoxy resin under vacuum. Vacuum removal of the soil air allows complete resin migration into the soil micropores. After resin polymerization, microscopic specimens that have cross-sectional areas of ~ 1 to 4 cm$^2$ were prepared for SEM examination by coarse sanding and fine polishing.

Mineralogical analyses by X-ray diffraction (XRD) of uranium-enriched size and density fractions of both soils were conducted to determine the nature of the uranium phases occurring in these soils. Phase identification was determined using the Joint Committee of Powder Diffraction Standards data base. Additionally, quantitative analysis on the carbonate minerals in these soils was performed by the reference intensity ratio (RIR) method (Chung 1974a, 1974b, 1975). The authors determined the RIR constants for dolomite, calcite, and quartz as well as the relative intensities of each pure mineral rather than using published values, because these constants strongly depend on the slide preparation for XRD. All XRD analyses were performed

on a Scintag 2000XDS equipped with CuK$\alpha$-radiation. Power settings for all XRD analyses were 45 kV and 40 ma. All diffractograms were collected from 2 to 70° 2$\Theta$ at 1° 2$\Theta$ $min^{-1}$.

## 2.3 EQUILIBRATION STUDY AND GEOCHEMICAL MODELING

For the equilibration study, 200 g of air-dried A-14 and B-16 soil were equilibrated with 2500 mL of deionized distilled water in a 1-gal polyethylene container. Duplicate samples of each soil and one experimental blank were also analyzed as an internal check on the precision of the analytical results and on the base-line quality of the water used in this study. For the first 10 weeks of the study, this mixture was shaken manually three times daily for 30 s each time and allowed to rest between these shakings. Periodically, these samples were also allowed to aerate to atmospheric conditions. After ten weeks, the samples were allowed to rest until the final sampling episode.

For each sampling episode, the samples were allowed to rest for 1 h following the first shaking before a 50-mL aliquot was taken from each sample. Each aliquot was then vacuum-filtered through 0.45-$\mu$m millipore membrane paper to remove all coarser particulates from the aliquot. Following filtration, the samples were brought to the analytical laboratory for immediate analysis of pH, dissolved cation and anions, total uranium, and alkalinity. Cation ($Na^+$, $Li^+$, $K^+$, $Ca^{2+}$, $Mg^{2+}$, $Fe^{3+}$, $Al^{3+}$, $Si^{4+}$, and many others) and anion ($Cl^-$, $F^-$, $NO_3^-$, $SO_4^{2-}$, $PO_4^{3-}$) concentrations were determined by inductively coupled plasma (ICP) spectroscopy and ion chromatography, respectively. Charge balance, based upon the analytical results, was used to check the performance of the analyses. A small average net positive charge of $1.52 \times 10^{-4}$ for soil A-14 and a small average net negative charge of $4.45 \times 10^{-4}$ for soil B-16 were calculated. Radionuclide concentrations ($^{235}U$ and $^{238}U$) and alkalinity were determined with the use of mass spectrometer and acid titration, respectively. Samples were taken according to the following schedule (in days after initial mixing): 1, 3, 7, 14, 21, 28, 70, and 300.

One caveat for this procedure is warranted. The withdrawal of 50-mL aliquots per sampling episode causes a reduction in the solution:solid ratio for each sampling episode of 2% of the initial solution volume. Initially, this ratio is 12.5:1, whereas at the end of the study the ratio is 10:1. Although extraction efficiencies are expected to become lower with lower solution:solid ratios, the authors believe that this ratio varies rather narrowly and is not expected to significantly retard the dissolution of these soils.

Geochemical modeling was performed using the Geochemical Expert System (GES) prototype (Hoffman and Tripathi 1993), a software system designed to analyze interactions between solution and mineral phases in nature. GES uses the MINEQL (Westall et al. 1976) equilibrium model to assess the rate and extent of geochemical interactions. GES then uses the results of the model to create qualitative geochemical interpretations similar to those written by expert geochemists. This program attempts to describe important characteristics and salient features of the prescribed geochemical composition using as much quantitative information obtained from the equilibrium model, as possible. GES actually generates English text to describe the state of oxidation/reduction, complexation, and precipitation/dissolution of the geochemical system.

Because of some assumptions made by GES, additional modeling was performed using MINEQL directly. These simulations were used to predict the complexation potential, activity, and degree of complexation of each dissolved species and the saturation indices of each solid phase. Kinetic processes were not modeled because kinetic data are uncertain or nonexistent.

# 3. RESULTS AND DISCUSSION

## 3.1 GENERAL SOIL PROPERTIES

The A-14 soil was covered by fescue grass. Soils near the concrete curb of the driveway were highly disturbed, but the soils away from the curb were less disturbed. This soil had a well-developed Ap horizon with a dark grayish-brown (7.5YR 4/2) color, 5% gravel content, high organic matter content, pH 7.2, and a silt loam texture. Undisturbed soils of this area are classified as the Fincastle soil series (USDA 1979).

The B-16 soil was also covered by fescue grass. In general, the soils near the Storage Pad were highly disturbed, but the soils away from the Storage Pad were less disturbed. This soil had a dark brown (7.5YR 3/3) color, 5% gravel content, pH 7.5, and a silt loam texture. These soil properties suggest that the B-16 soil may be similar to the Ap horizon of the Henshaw soil series (USDA 1979).

Even though soils A-14 and B-16 share the same textural class, differences in the actual percentages for each fraction are evident. The A-14 soil has a greater silt percentage and lesser sand and clay percentages than the spatially adjacent B-16 soil (Table 1).

**Table 1. Results of particle size and uranium distribution of the soils equilibrated**

| | | Size range | Size distribution | Uranium concentration | Uranium contribution | |
|---|---|---|---|---|---|---|
| Soil | Class | mm | (%) | mg/kg | mg/kg | (%) |
| A-14 | Gravel | >2 | 5 | <1 | <1 | <1 |
| | Sand | 2-0.05 | 12 | 1043 | 125 | 27 |
| | Silt | 0.05-0.002 | 70 | 288 | 203 | 44 |
| | Clay | <0.002 | 13 | 1026 | 133 | 29 |
| B-16 | Gravel | >2 | 5 | <1 | <1 | <1 |
| | Sand | 2-0.05 | 21 | 117 | 25 | 7 |
| | Silt | 0.05-0.002 | 54 | 240 | 129 | 37 |
| | Clay | <0.002 | 20 | 989 | 195 | 56 |

## 3.2 NATURE OF URANIUM CONTAMINATION

The uranium partitioning among the particle-size fractions of both soils is shown in Table 1. The distribution of uranium among the particle-size fractions indicates that the nonclay fractions contain most of the uranium in soil A-14 and 44% of the uranium in soil B-16. The results are conclusive evidence that the uranium in these soils mainly occurs as a particulate form rather than

an adsorbed form on the external and internal surfaces of layer silicate minerals (clay minerals). SEM analyses of the samples also confirm this interpretation (Plates 1 and 2).

Results of the heavy liquid separations for both soils show a predominance of light minerals over heavy minerals (Table 2). For both A-14 silt and sand, >96% of the total sample occurred in the light fraction. For B-16 silt, >80% of the sample occurred in the light fraction. For B-16 sand, the figure rose to 96%.

Results of the uranium partitioning among all particle density fractions show much higher levels of uranium phases (on an equivalent weight basis) in A-14 than B-16. Furthermore, higher uranium levels were associated with the sand fractions than with the silt fractions of each soil. A predominance of uranium phases was observed in the heavy sand and silt fractions of A-14, and the highest levels of uranium of any density fraction were observed in the heavy sand fraction of this soil. Nearly equal uranium levels were observed between the light and heavy fractions of B-16, thereby indicating an ineffective density separation for this sample. All uranium-rich heavy fractions were later examined by XRD for determination of their uranium mineralogy.

**Table 2. Results of the uranium partitioning among the particle density fractions of the equilibrated soils**

| Soil | Size fraction | Weight distribution | | Density fraction | |
|---|---|---|---|---|---|
| | | Heavy | Light | Heavy | Light |
| | | -------%-------- | | --------pCi/g-------- | |
| A-14 | Silt | 2 | 98 | 516 | 34 |
| | Sand | 4 | 96 | 1740 | 414 |
| B-16 | Silt | 21 | 80 | 15 | 21 |
| | Sand | 4 | 96 | 40 | 37 |

## 3.3 MINERALOGICAL PROPERTIES

SEM micrographs of the A-14 sand fraction show a wide variety of sizes and shapes of minerals (Plate 1). Some minerals occur as a stable, large-sized aggregate. The unusually high stability of the aggregates is expected to develop during the incinerating process. The aggregates contained uranium particles as well as other heavy minerals. Uranium occurred also as a microfracture-filling mineral in the aggregate. Uranium-containing particles were typically composed of calcium, silicon, or phosphorus. A cerium phosphate mineral was also found in this sample. Quartz was the dominant mineral in the sand fraction.

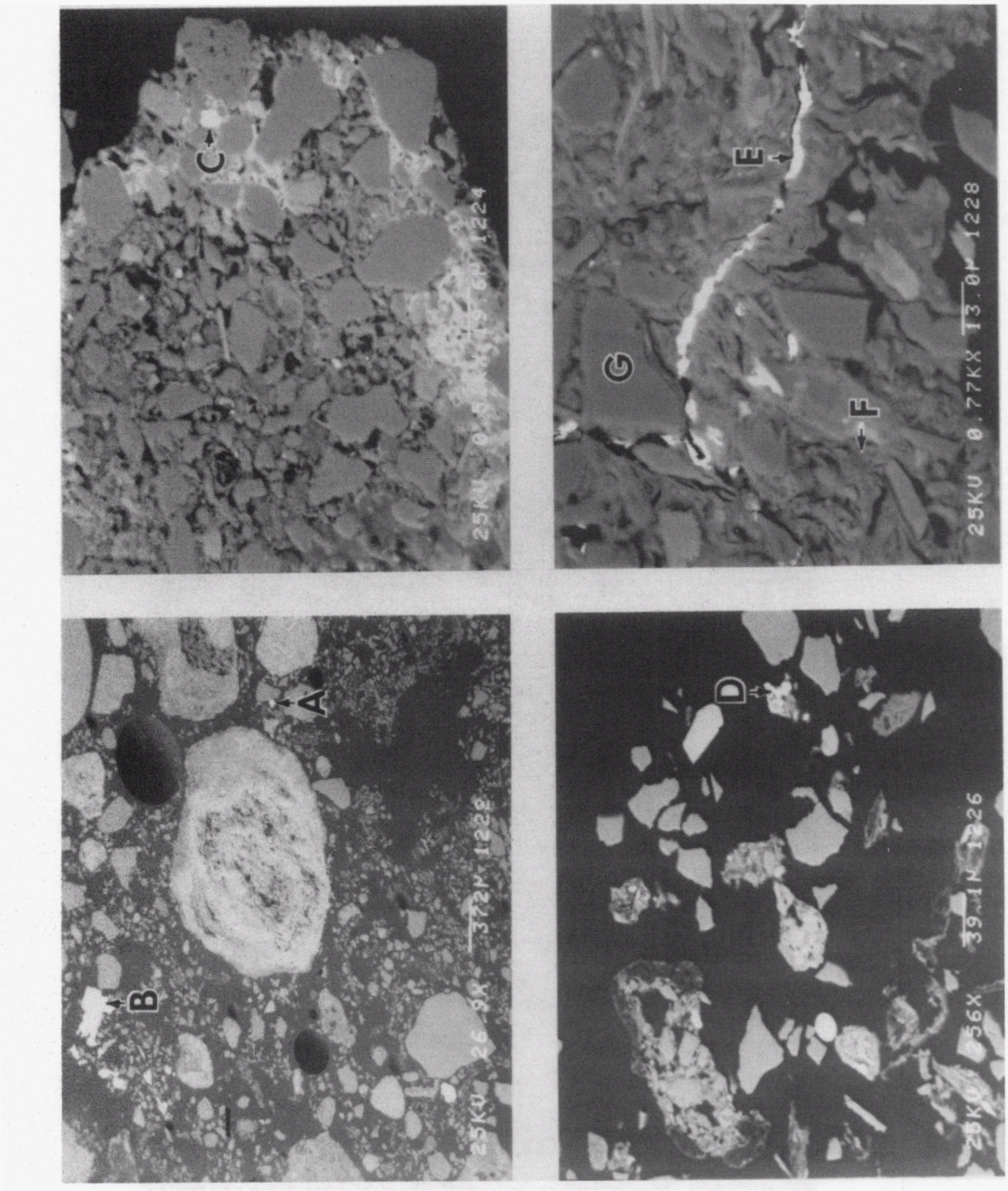


Plate 1. Four scanning electron micrographs were taken from the sand fraction of the A-14 sample. Particle A has uranium as a major component and a small amount of oxygen. Particles B and D have uranium and a lesser amount of calcium, phosphorus, and oxygen. Particle C has phosphorus, cerium, neodymium, and a lesser amount of thorium and oxygen. The microfracture-filling mineral (marked E) has uranium, silicon, and a smaller amount of calcium and phosphorus. The matrix of the aggregate is aluminosilicate clays (marked F) and silt-size quartz (marked G).

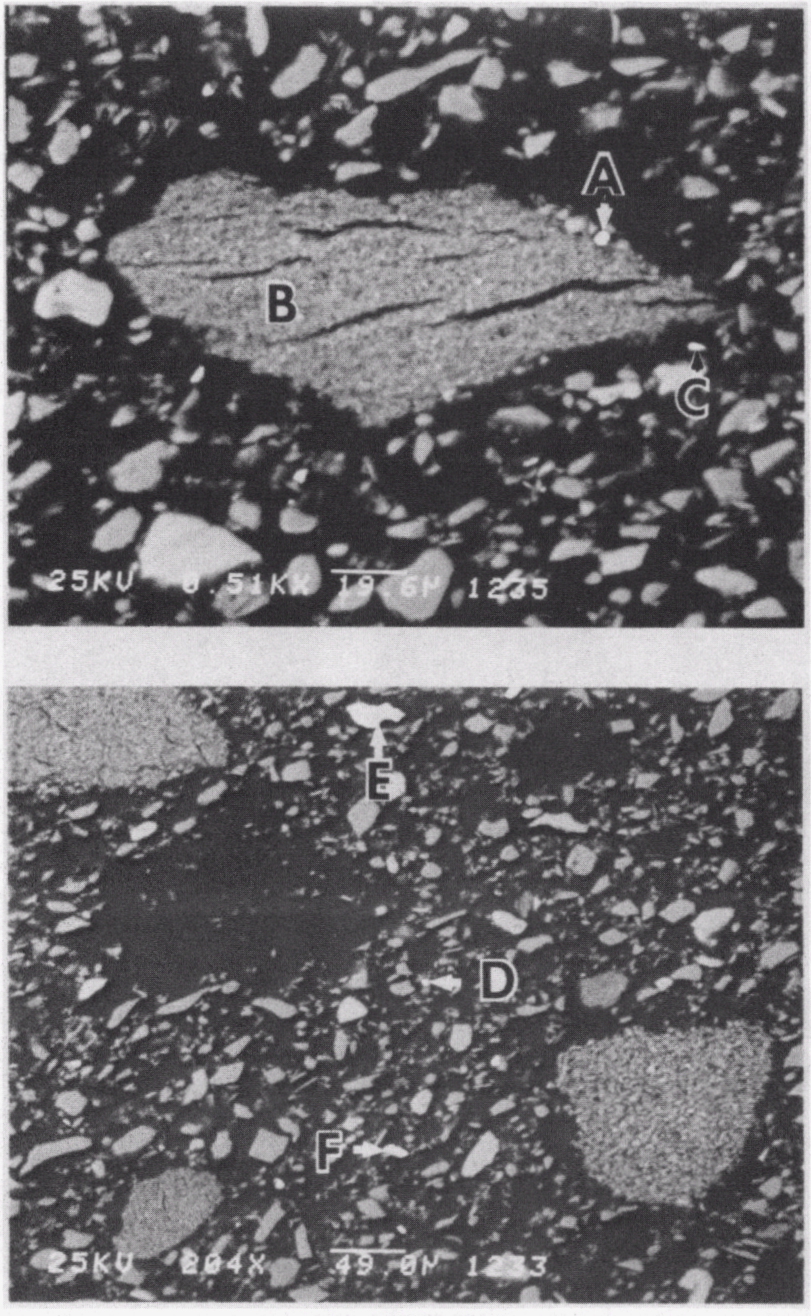


Plate 2. Two scanning electron micrographs were taken from the silt fraction of the B-16 sample. The uranium particle A also contains calcium, silicon, and aluminum. The fine silty aggregate is an aluminosilicate mineral (marked B). Particle C is an iron oxide mineral and particle D is a phosphate mineral that contains cerium, neodymium, and lanthanum (possibly monazite mineral). Particles E and F are an iron/titanium oxide (ilmenite) mineral. Other silt particles are quartz, dolomite (marked G), and feldspars.

In the B-16 silt fraction (Plate 2), uranium particles either were composed entirely of uranium or coexisted with calcium and/or silicon. In future analytical determinations, detailed microscopic analyses will be performed after heavy liquid separation in order to examine concentrated uranium-bearing fractions.

Mineralogically, these two soils are dominated by quartz and carbonate minerals in their bulk soil. Calcite [$CaCO_3$] and dolomite [$CaMg(CO_3)_2$] have been identified as the carbonate minerals in these soils. These two carbonate minerals are anthropogenic artifacts because these two minerals are not present in the nearby off-site soils at this same depth. They occur in these soils because FEMP personnel placed these minerals on the uranium-contaminated soils for erosion control and road construction activities. Quantitative estimates of the carbonate minerals and quartz on a whole soil basis are 20% calcite, 2% dolomite, 65% quartz, and 13% clay minerals in soil A-14 and 15% calcite, 19% dolomite, 46% quartz, and 20% clay minerals in soil B-16. Feldspars were minor phases in both soils. Kaolinite and illite are the two most dominant clay-sized minerals, and lesser amounts of quartz and traces of smectite and/or vermiculite occur in this size fraction of both soils.

In terms of uranium mineralogy, uraninite [$UO_2$] is the only uranium mineral identified in these soils. This mineral was observed only in the heavy-sand nonmagnetic fraction of core SP-9, which was sampled in the same area as soil A-14. This tetravalent form of uranium is much less soluble than the hexavalent form and may be partly responsible for the lower extraction efficiencies of the A-14 soil than the B-16 soil as reported by the leaching task group (Francis et al. 1992). Other minerals observed in the heavy-sand and silt fractions of both soils include amphiboles, anatase, and iron oxides.

## 3.4 EQUILIBRATION STUDY AND GEOCHEMICAL MODELING

Results showed that the soluble levels of the major components (total uranium, calcium, magnesium, nitrate, and carbonate) continually increased for the first 28 d and then either approached a steady-state condition in those components having solubilities nearing that of the controlling solid phase for that component or continued linearity throughout the study in those components having low solubilities. Other major components, such as aluminum, potassium, and iron, reached a steady-state concentration within 3 d. Silica levels approximated the predicted solubility of quartz throughout the study.

On average, total uranium levels increased linearly throughout the study from $<0.1$ to 3.8 mg U/L ($<1$ to 36 $\mu$g U/g soil) in soil A-14 <Fig. 1a>. The maximum concentration represents only 7% of the total uranium in the whole soil of A-14. A similar increase along a logarithmic function from 2.5 to 10.0 mg U/L (30 to 95 $\mu$g U/g soil) was observed for the B-16 soil <Fig. 1b>. This maximum concentration represents 21% of the total uranium in the whole soil of B-16.

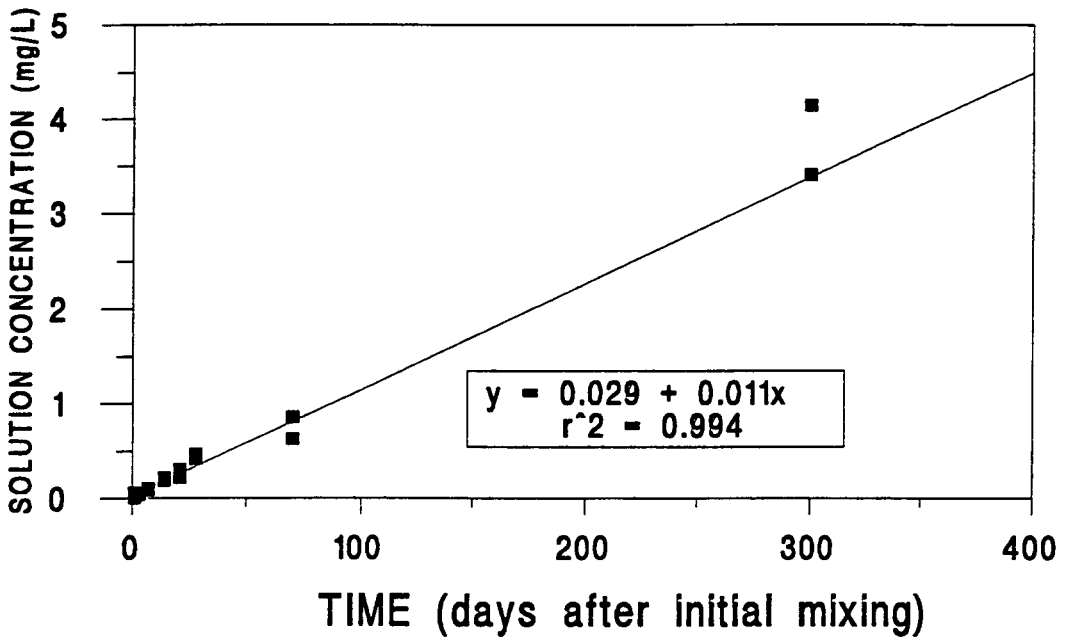


(a)

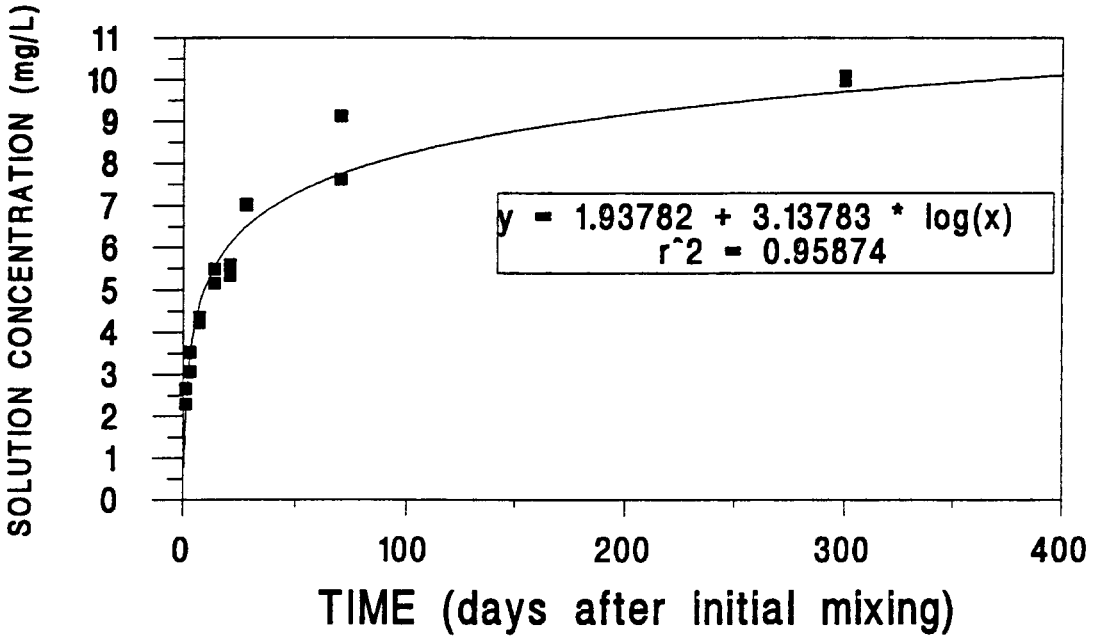


(b)

Fig. 1. Total soluble uranium concentrations versus time for (a) soil A-14 and (b) soil B-16. Data for both duplicates are shown.

Quite evidently, much higher absolute and relative levels of soluble uranium were observed throughout the study in the B-16 than the A-14 soil. In fact, the uranium concentration in B-16 soil solution after 300 d is nearly three times the corresponding uranium concentration in A-14 soil solution. The low-soluble uranium levels observed for soil A-14 cause this soil to remain undersaturated with respect to the uranium minerals considered by MINEQL in this study. The linearity in uranium solubility for soil A-14 indicates that saturation with respect to uranium minerals has not been approached in this soil. In soil B-16, the much higher levels appear to approach a steady-state condition, suggesting that saturation or near saturation with respect to uranium minerals has been reached. The overall greater solubility of uranium in the B-16 soil may be due to the higher carbonate content of this soil compared with that of A-14 and to the presence of less soluble tetravalent uranium-bearing refractive phases (i.e., uraninite) formed in the incinerating process in soil A-14.

Calcium and magnesium were the two dominant soluble cationic species observed throughout this study. For the A-14 soil, calcium levels increased along a logarithmic function from 8.7 to 31.8 mg/L (107 to 325 $\mu$g Ca/g soil) before decreasing to 30.9 mg/L (294 $\mu$g Ca/g soil) at 300 d, whereas magnesium levels increased along a logarithmic function from 2.0 to 6.2 mg/L (25 to 63 $\mu$g Mg/g soil) before decreasing to 4.1 mg/L (39 $\mu$g Mg/g soil) at 300 d <Fig. 2a>. For the B-16 soil, calcium levels increased rapidly along a logarithmic function from 19.0 to 36.0 mg/L (232 to 397 $\mu$g Ca/g soil) through the first 4 weeks and afterward have been nearly constant through 300 d. Magnesium behaved similarly; levels also increased along a logarithmic function from 2.9 to 5.1 mg/L (36 to 56 $\mu$g/g soil) through the first 4 weeks and afterward have been nearly constant through 300 d <Fig. 2b>. The nearly constant calcium and magnesium levels after 28 d in both soils is interpreted as the attainment of saturation or near-saturated conditions with respect to the controlling calcium and magnesium phases in this soil. Other soluble cationic species (i.e., sodium, iron, and aluminum) remained at low concentrations throughout the study in both soils (see Appendix). The slightly higher concentrations of soluble calcium and magnesium in soil B-16 probably reflect the higher calcite and dolomite mineral contents in this soil than those in soil A-14.

Total carbonate species or alkalinity was the dominant anionic species throughout the study for both soils. Bicarbonate was the dominant carbonate species present throughout the study. For soil A-14, total soluble bicarbonate levels increased along a logarithmic function from 13.0 to 81.5 mg/L (159 to 774 $\mu$g/g soil) <Fig. 3a>. For soil B-16, total soluble bicarbonate levels increased along a logarithmic function from 39.5 to 110.0 mg/L (484 to 1045 $\mu$g/g soil) <Fig. 3b>. The logarithmic response of alkalinity for both soils signifies an approach to saturated conditions with respect to the controlling carbonate species. The observed increase in the total uranium levels with increasing carbonate levels is very likely due to the enhanced solubility and complexation of uranium by carbonate species.

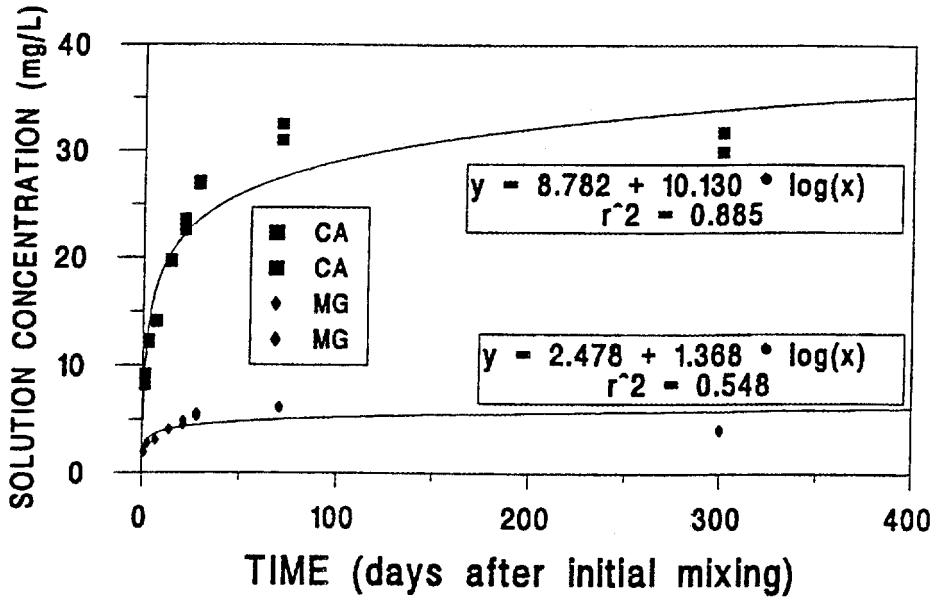


(a)

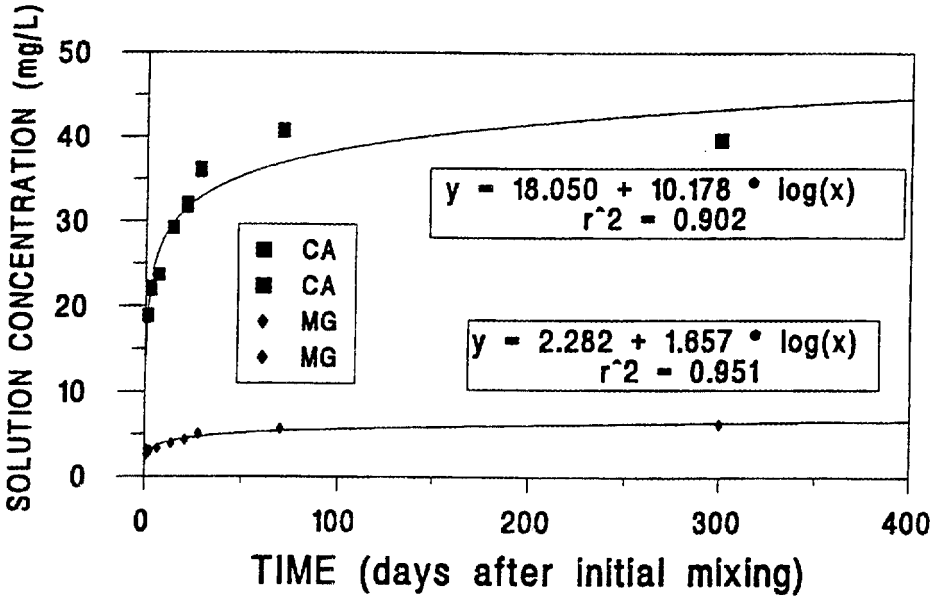


(b)

Fig. 2. Total soluble calcium and magnesium concentrations versus time for (a) soil A-14 and (b) soil B-16. Data for both duplicates are shown.

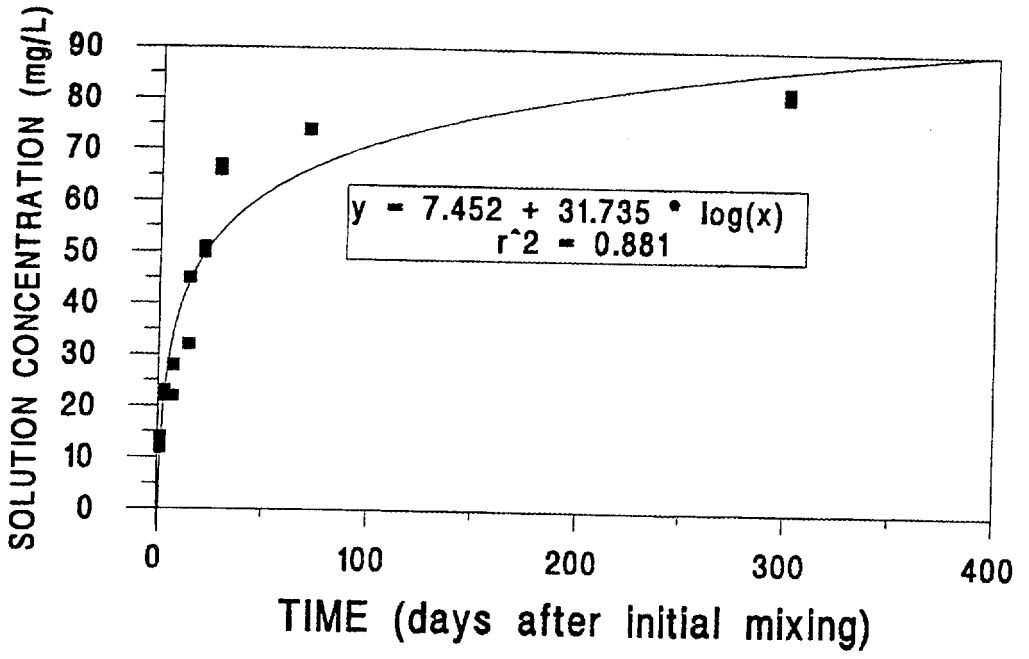


(a)

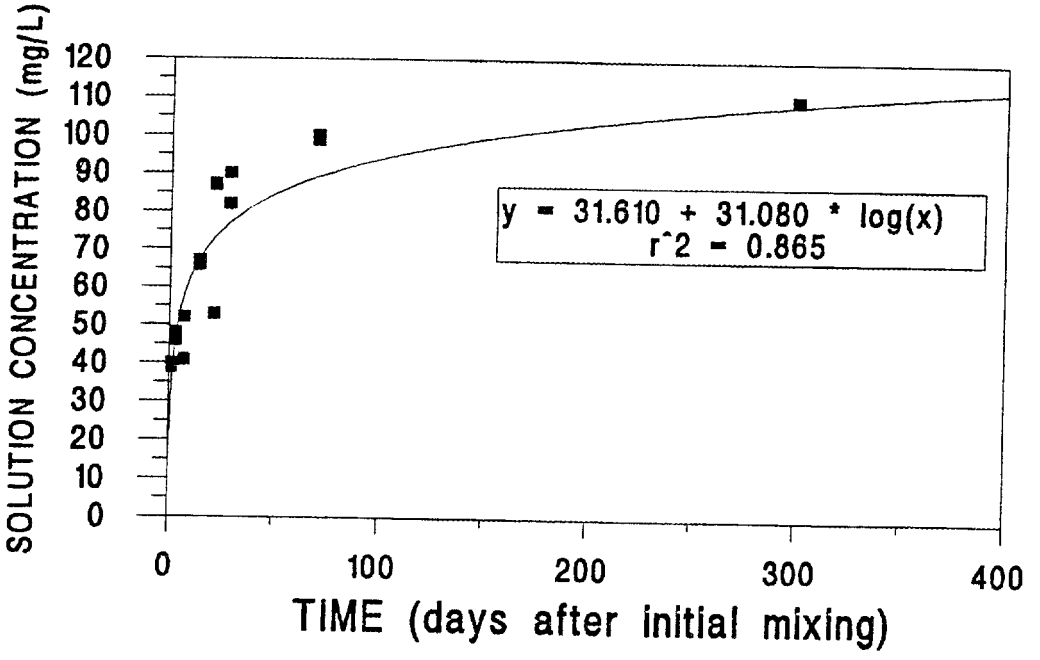


(b)

Fig. 3. Total soluble alkalinity concentration versus time for (a) soil A-14 and (b) soil B-16. Data for both duplicates are shown.

Nitrate was the next dominant anionic species. Overall, nitrate levels generally increased logarithmically through the first 10 weeks in both soils, and slightly higher levels were observed in the A-14 soil <Figs. 4a, 4b>. After 10 weeks until the final sampling at 300 d, nitrate levels dropped precipitously to <25% of the maximum levels for both soils. The authors believe that the microorganisms depleted the dissolved oxygen in the closed containers from a 70- to 300-d period. Anaerobic bacteria (either chemoautotrophs or chemoheterotrophs) would then use nitrate as their electron sink and dramatically lower nitrate levels. The presumed lowering of the pe may be responsible for the increase in pH (>8.0 for both soils) during this final sampling episode because of the inverse relationship of pe and pH in the Nernst equation (Ponnamperuma 1972). This pH increase may in turn induce calcite precipitation in these soils which may account for the observed evening to lowering of both the calcium and magnesium levels with time. Excluding the levels associated with the 300-d sampling episode, sulfate concentrations similar to those of nitrate were observed in the B-16 soil; however, sulfate levels in the A-14 soil remained quite low (see Appendix). This observed anaerobicity is unlikely to occur in the field because these soils are seldom saturated for long periods of time to induce anaerobic conditions. The extension of the best-fit line in these two graphs beyond the first 10 weeks is suspect; however, the authors believe that this logarithmic extension, which assumes little to no anaerobic conditions occurring in these soils, more accurately models the natural situation of these soils. Other soluble anionic species (i.e., chloride, fluoride, and phosphate) remained at low concentrations throughout the study in both soils (see Appendix).

In terms of pH, both soils showed a rapid increase in pH within the first 3 d and then achieved a steady-state condition through the first 10 weeks of the study. Both soils, however, showed a strong increase in pH (>0.5 pH unit increase) at the 300-d sampling episode (see Appendix). As stated earlier, this pH increase may be related to the observed nitrate reduction process, which occurred within these closed containers from 70 to 300 d. Reduction processes are known to consume excess protons, causing a concomitant increase in pH. One potential ramification of increasing pH may be calcite precipitation, which lowers soluble calcium, alkalinity, and even magnesium levels. The more alkaline pH at the start of the study in soil B-16 than in soil A-14 probably reflects the higher carbonate mineral content of this soil.

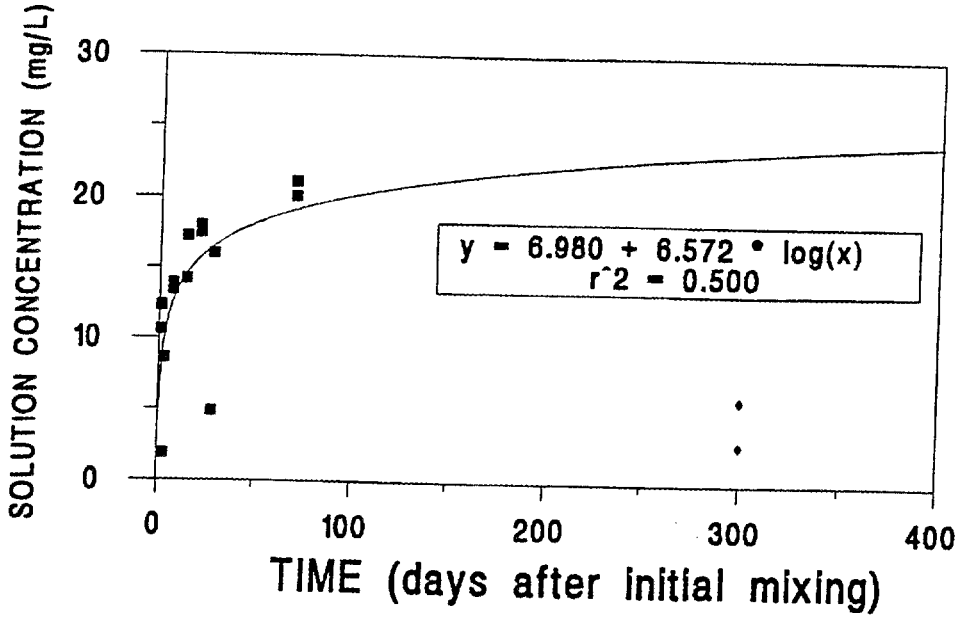


(a)

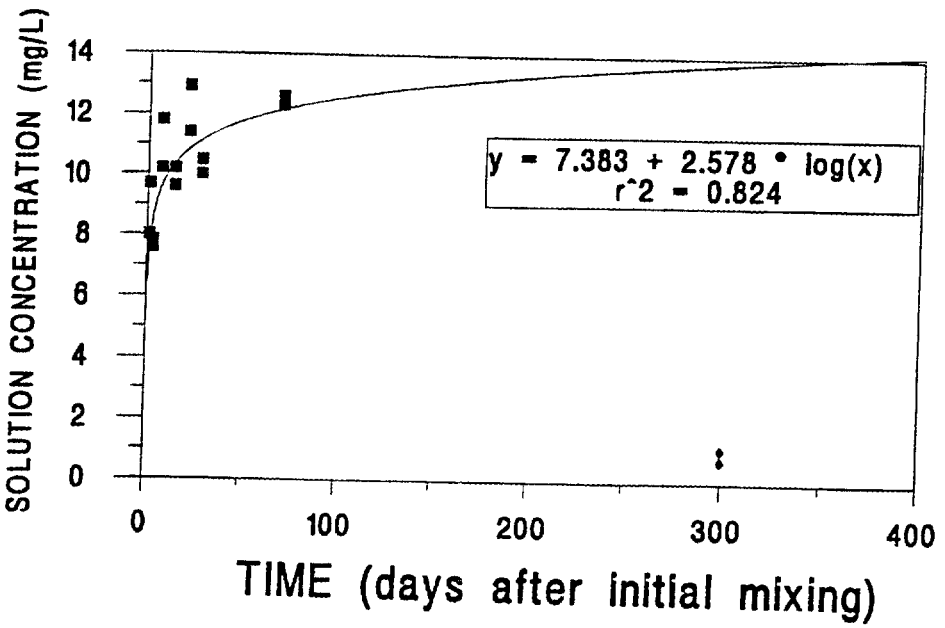


(b)

Fig. 4. Total soluble nitrate concentrations versus time for (a) soil A-14 and (b) soil B-16. Data for both duplicates are shown. Best-fit line excludes 300 d data points.

Geochemical modeling was employed to determine the complexation potential of soluble uranium. Given that the pH for both soils is near neutral, the redox potential of the soil solutions was assumed to be zero voltage. This is also a conservative estimate based upon the typical Eh–pH pairs found in natural aqueous environments (Garrels and Christ 1965). This estimate is not a critical factor for the uranium speciation results because the most important uranium redox couples occur at even more oxidizing conditions than the assumed condition (Garrels and Christ 1965). Results indicate that the three most dominant soluble uranium species for both soils were uranyl dicarbonate $[UO_2(CO_3)_2]^{2-}$, uranyl tricarbonate $[UO_2(CO_3)_3]^{4-}$, and trihydroxocarbonatodiuranyl $[(UO_2)_2CO_3(OH)_3]^{1-}$. Uranyl dicarbonate accounted for 55% of the total dissolved uranium, whereas uranyl tricarbonate and trihydroxocarbonatodiuranyl accounted for 27% and 9% of the total dissolved uranium, respectively, for soil A–14. Similarly for soil B–16, uranyl dicarbonate accounted for 40% of the total dissolved uranium, whereas uranyl tricarbonate and trihydroxocarbonatodiuranyl accounted for 30% and 13%, respectively. It is important to note that among these three most dominant soluble uranium species, anionic uranium species account for 91 and 83% of the total soluble uranium species in soils A–14 and B–16, respectively. Therefore a large portion of the uranium solubilized in this experiment is calculated to be in an anionic form that would be quite mobile in the soil environment and would possibly contaminate the underlying groundwater.

**Table 3. Comparison of the average major chemical components between the two Fernald soils after equilibrium and the groundwater wells at the Fernald site. Concentrations of all dissolved species, excluding pH, are in milligrams per liter.**

| Dissolved species | Equilibration data A–14 | B–16 | Groundwater High | Low |
|---|---|---|---|---|
| pH | 8.0 | 8.2 | 7.5 | 6.6 |
| Calcium | 31 | 40 | 261 | 92 |
| Magnesium | 4 | 6 | 75 | 36 |
| Alkalinity | 82 | 110 | 323 | 214 |
| Uranium | 4 | 10 | 12 | 1 |
| Major uranium species | $[UO_2(CO_3)_2]^{2-}$ $[UO_2(CO_3)_3]^{4-}$ $[(UO_2)_2CO_3(OH)_3]^{1-}$ | | $[UO_2(CO_3)_2]^{2-}$ $[UO_2(CO_3)_3]^{4-}$ $[(UO_2)_2CO_3(OH)_3]^{-1}$ | |

Similar ranges in pH and total uranium were observed between the two Fernald soils and the groundwater (Tidwell et al. 1992). Additionally, similar aqueous uranium species predicted to occur in this study were also predicted to occur in the groundwater wells at the Fernald site <Tab 3>. However, much higher levels of soluble calcium, magnesium, and total carbonate were observed in the groundwater wells at the site. This direct comparison of the soil solution results with the groundwater results is tentative because (1) the solution:soil ratio associated with the groundwater is unknown, (2) the recharge/discharge behavior of the groundwater is also unknown, and (3) the transient character or "seasonality" of the groundwater was not modeled in this study.

The water chemistries from this study were also used to predict undersaturation, equilibrium, and supersaturation conditions with respect to chemically similar minerals. The water chemistries at steady state of both soils were either near equilibrium or supersaturated with respect to uraninite [$UO_2$], calcium autunite [$Ca(UO_2)_2(PO_4)_2$], fluorapatite [$Ca_5(PO_4)_3F$], hydroxyapatite [$Ca_5(PO_4)_3OH$], calcite [$CaCO_3$], dolomite [$CaMg(CO_3)_2$], and quartz. The water chemistries at steady state of both soils were undersaturated with respect to sodium autunite [$Na_2(UO_2)_2(PO_4)_2$] and ningyoite [$UCa(PO_4)_2*2H_2O$]. It is interesting to note that the majority of the minerals predicted to be near equilibrium or supersaturated are phosphate minerals. Because the uranium incorporated into calcium phosphate minerals is insoluble, the phosphate concentration controls the rate of uranium release from these minerals. Therefore, the phosphate concentration may be considered the master variable in influencing the dissolution behavior of the Fernald soils.

Thermodynamically, $UO_2(HPO_4)_2^{2-}$ is the most soluble uranyl species between pH 4 and 7.6, whereas $UO_2(CO_3)_2^{2-}$ and $UO_2(CO_3)_3^{4-}$ become the most soluble uranyl species above pH 7.6 in a purely aqueous system (Langmuir 1978). However, in soil-solution systems, phosphate anions readily adsorb onto the surfaces of minerals that are pH dependently charged (i.e., kaolinite and sesquioxides) (Lindsay et al. 1989). Adsorption of phosphate reduces its availability in the soil solution and causes the dominance of uranyl-carbonate complexes in both soils.

Tidwell et al. (1992) found that the water chemistries from all six groundwater wells investigated at the Fernald site showed supersaturation with respect to soddyite [$(UO_2)_2SiO_42H_2O$]. Additionally, four of these wells showed saturation with respect to haiweeite [$Ca(UO_2)_2Si_6O_{15}5H_2O$], whereas the other two were slightly undersaturated with respect to haiweeite. In one well, that contained the highest phosphate levels, supersaturation with respect to $(UO_2)_3(PO_4)_24H_2O$) and saleeite [$(UO_2)_2Mg(PO_4)_2$] was observed. Rutherfordine [$UO_2CO_3$] and schoepite were also observed near saturation in all wells. Supersaturation with respect to uranium silicate minerals at equilibrium in their groundwater wells was predicted because they assume silicon saturation with respect to quartz in the well waters.

The observed dissolution behavior of both Fernald soils was used to estimate the leaching of uranium from these soils under natural conditions (i.e., a severe or prolonged storm event). Linear regression analysis using soluble uranium levels during the first 3 d of this study was performed to determine the expected level of uranium solubilized under these conditions. This estimate is conservative because the uranium values during the first 3 d for both soils are undersaturated with respect to any uranium-bearing mineral. Additionally, some uranium-bearing

pore water is still held in the soil even after a storm. Even upon uranium precipitation during the next dry cycle, this freshly precipitated form would be much more easily redissolved in the next wet cycle as a uranyl carbonate form rather than initially when it is not bound with carbonate. Results of this analysis predict that 0.4 $\mu$g U/g soil (0.09%) and 15.6 $\mu$g U/g soil (4.47%) would become solubilized for A-14 and B-16, respectively. Because the mode of uranium contamination associated with soil B-16 represents the typical mode of uranium contamination at the Fernald site, the higher predicted soluble uranium levels associated with soil B-16 impart severe ramifications for groundwater contamination at the Fernald site. If this solubilized uranium does not become readsorbed onto soil particles, significant contamination of the groundwater underlying this soil will result.

# 4. SUMMARY AND RECOMMENDATIONS

Results from a 300-d equilibration study involving two uranium-contaminated soils from the DOE Fernald site have predicted that the solubilized uranium exists mainly as anionic uranyl-carbonate species. Because of their anionic character, these species are considered quite mobile in the soil environment and may contaminate the underlying groundwater under prolonged and/or severe leaching conditions. High levels of soluble calcium, magnesium, and bicarbonate are probably the result of the dissolution of magnesium and\or calcium carbonate minerals in these soils. The increase of carbonate levels in the solute by progressive dissolution of the minerals would enhance the solubility of uranium-bearing minerals by carbonate complexation on the surface of the particulates.

The implication of this work is very important in many ways. For example, uranium transport assessment to off-site areas as a part of risk assessment should recognize that the solubility of uranium-bearing minerals is the critical factor rather than uranium distribution coefficient (Kd) in soils. Anionic uranyl-carbonate complexes are very stable in this carbonate-dominated system (i.e. carbonate-rich soil, parent material, and groundwater). Therefore, as long as the pH of these soils is maintained near neutrality, sorption of uranium onto soil particles will be unlikely in both Fernald soils. FEMP site management should realize that the use of carbonate minerals on these soils for the control of erosion and for road construction activities actually aids in the leaching of uranium from contaminated soil particles. The dissolved carbonates promote uranium solubility, forming highly mobile anionic species. Unfortunately, such contamination has been documented in groundwater wells at the Fernald site. Therefore, the development of a site-specific remediation technology is urgently needed for the FEMP site.

# 5. LITERATURE CITED

Bowie, S. H. U., and J. A. Plant. 1983. Natural radioactivity in the environment. pp.481-94. In I. Thornton (ed.), Applied Environmental Geochemistry. Academia Press, New York.

Chung, F. H. 1974a. Quantitative interpretation of X-ray diffraction patterns. I. Matrix-flushing method of quantitative multicomponent analysis. J. Appl. Crystallogr. 7:519-25.

Chung, F. H. 1974b. Quantitative interpretation of X-ray diffraction patterns. II. Adiabatic principle of X-ray diffraction analysis of mixtures. J. Appl. Crystallogr. 7:526-31.

Chung, F. H. 1975. Quantitative interpretation of X-ray diffraction patterns. III. Simultaneous determination of a set of reference intensities. J. Appl. Crystallogr. 8:17-19.

Garrels, R. M., and C. L. Christ. 1965. Solutions, Minerals, and Equilibria. Freeman, Cooper, and Company, San Francisco.

Hoffman, F. M., and V. S. Tripathi. 1993. A geochemical expert system prototype using object-oriented knowledge representation and a production rule system. Comput Geosci. 19(1):53-60.

Jackson, M. L. 1975. Soil Chemical Analysis-Advanced Course. Published by the author, Dept. of Soil Science, University of Wisconsin, Madison.

Kneff D. W., G. Subbaraman, and R. J. Tuttle. 1992. Homogeneity evaluation of Fernald soils prepared for treatability studies. ETEC/GEN-ZR-0018. Energy Technology Engineering Center, Rocketdyne Division, Rockwell International, Los Angeles.

Langmuir, D. 1978. Uranium solution-mineral equilibria at low temperatures with applications to sedimentary ore deposits. Geochim. Cosmochim. Acta 42:547-69.

Larsen, I. L., S. Y. Lee, H. L. Boston, and E. A. Stetar. 1992. Discovery of a $^{137}Cs$ hot particle in municipal wastewater treatment sludge. Health Phys. 62(3):235-38.

Lee, S. Y., and J. D. Marsh, Jr. 1992. Characterization of uranium contaminated soils from DOE Fernald Environmental Management Project Site: Results of Phase I characterization. ORNL/TM-11980. Oak Ridge National Laboratory.

Lindsay, W. L., T. L. G. Vlek, and S. H. Gnichien. 1989. Phosphate minerals. pp. 1089-1130. In J. B. Dixon and S. B. Weed (eds.), Minerals in Soil Environments. Second edition. American Society of Agronomy, Madison, Wisconsin.

Ponnamperuma, F. N. 1972. The chemistry of submerged soils. Adv. Agron. 24:29-96.

Tidwell, V. C. et al. 1992. An integrated approach to the characterization of uranium-contaminated soils. In Spectrum 92: Proceedings of Nuclear and Hazardous Waste Management. American Nuclear Society, Boise, Idaho.

USDA. 1979. Soil Survey of Hamilton County, Ohio. Soil Conservation Service, U.S. Department of Agriculture, Washington, D.C.

Wade, J. W., F. F. Dyer, L. Robinson, N. A. Teasley, and J. R. Stokely. 1992. Neutron activation analysis of East Fork Poplar Creek samples. AC-MM-222002. Oak Ridge National Laboratory.

Westhall, J. C., J. L. Zachary, and F. M. M. Morel. 1976. MINEQL: A Computer Program for the Calculation of Chemical Equilibrium Composition of Aqueous Systems. Massachusetts Institute of Technology, Cambridge, Massachusetts.

# APPENDIX

Soil Equilibration Results of the Major Cations

Soil Equilibration Results of the Major Anions

Soil Equilibration Results of the Major Cations

| Sample | Sampling Period | Sampling Volume | pH | Total Uranium | Al | Ca | Fe | Si | Mg | Na |
|---|---|---|---|---|---|---|---|---|---|---|
| | days | mL | | <-----mg/L-----> | | | | | | |
| A-14 | 1 | 2450 | 6.6 | 0.035 | 1.10 | 8.70 | 0.90 | ND | 2.00 | 1.10 |
| | 3 | 2400 | 6.9 | 0.050 | 1.40 | 12.25 | 1.10 | ND | 2.80 | 1.85 |
| | 7 | 2350 | 6.9 | 0.098 | 0.35 | 14.15 | 0.25 | ND | 3.10 | 0.75 |
| | 14 | 2300 | 7.7 | 0.205 | 0.25 | 19.70 | 0.30 | 3.10 | 4.10 | 2.10 |
| | 21 | 2250 | 6.9 | 0.260 | 0.20 | 23.10 | 0.15 | 4.25 | 4.70 | 0.65 |
| | 28 | 2200 | 7.3 | 0.443 | BDL | 27.05 | BDL | ND | 5.45 | 0.90 |
| | 70 | 2050 | 7.1 | 0.743 | 1.05 | 31.75 | 0.85 | 6.00 | 6.15 | 0.95 |
| | 300 | 1900 | 8.0 | 3.780 | BDL | 30.90 | BDL | 4.50 | 4.10 | 1.00 |
| B-16 | 1 | 2450 | 7.6 | 2.480 | 1.85 | 18.95 | 1.75 | ND | 2.90 | 2.30 |
| | 3 | 2400 | 7.4 | 3.290 | BDL | 22.15 | BDL | ND | 3.05 | 2.25 |
| | 7 | 2350 | 7.4 | 4.295 | BDL | 23.75 | BDL | ND | 3.30 | 2.00 |
| | 14 | 2300 | 7.9 | 5.325 | BDL | 29.25 | BDL | 2.45 | 3.95 | 2.20 |
| | 21 | 2250 | 7.4 | 5.470 | BDL | 31.90 | BDL | 3.00 | 4.35 | 1.85 |
| | 28 | 2200 | 7.7 | 7.020 | BDL | 36.05 | BDL | ND | 5.05 | 2.15 |
| | 70 | 2050 | 7.7 | 8.370 | BDL | 40.70 | BDL | 3.00 | 5.65 | 2.10 |
| | 300 | 1900 | 8.2 | 10.040 | BDL | 39.75 | BDL | 3.90 | 6.25 | 2.45 |

Note: BDL = Below detection limit (For Al, BDL < 0.2 mg/L. For Fe, BDL < 0.3 mg/L).
ND = Not determined.

Soil Equilibration Results of the Major Anions

| Sample | Sampling Period | Sampling Volume | Cl | F | NO3 | PO4-P | SO4 | TOTAL ALK |
|---|---|---|---|---|---|---|---|---|
| | days | mL | <-----mg/L-----> | | | | | |
| A-14 | 1 | 2450 | 1.02 | 0.58 | 11.45 | 1.17 | 1.89 | 13.00 |
| | 3 | 2400 | 1.93 | 1.83 | 5.25 | 0.29 | 2.18 | 22.50 |
| | 7 | 2350 | 0.57 | 1.97 | 13.65 | BDL | 2.75 | 25.00 |
| | 14 | 2300 | 2.19 | 1.99 | 15.70 | BDL | 3.88 | 38.50 |
| | 21 | 2250 | 0.82 | 1.90 | 17.75 | 4.01 | 3.77 | 50.50 |
| | 28 | 2200 | 0.78 | 1.10 | 10.45 | 2.95 | 2.80 | 66.50 |
| | 70 | 2050 | 1.38 | 0.97 | 20.60 | 4.20 | 3.87 | 74.00 |
| | 300 | 1900 | 2.92 | 1.52 | 4.39 | 2.52 | 4.70 | 81.50 |
| B-16 | 1 | 2450 | 1.36 | 2.59 | 8.86 | BDL | 8.71 | 39.50 |
| | 3 | 2400 | 0.90 | 3.39 | 7.72 | BDL | 7.51 | 47.00 |
| | 7 | 2350 | 0.50 | 6.43 | 11.00 | BDL | 9.33 | 46.50 |
| | 14 | 2300 | 0.52 | 8.09 | 9.91 | BDL | 9.74 | 66.50 |
| | 21 | 2250 | 0.80 | 8.24 | 12.15 | BDL | 10.95 | 70.00 |
| | 28 | 2200 | 0.54 | 4.10 | 10.25 | BDL | 9.35 | 86.00 |
| | 70 | 2050 | 0.93 | 3.62 | 12.45 | BDL | 12.65 | 99.50 |
| | 300 | 1900 | 4.07 | 3.95 | 0.92 | 0.29 | 18.40 | 110.00 |

Note: BDL = Below detection limit. For $PO_4$, BDL < 0.125 mg/L.

## Internal Distribution List

1. H. L. Adair
2. M. R. Ally
3. A. R. Armstrong
4. M. L. Baker
5. J. B. Berry
6. H. L. Boston
7. C. H. Brown
8. N. H. Cutshall
9. T. L. Donaldson
10. N. T. Edwards
11-20. M. P. Elless
21. C. J. Ford
22-24. C. W. Francis
25. D. D. Gates
26. J. R. Hightower
27. S. G. Hildebrand
28-37. F. Hoffman
38-47. S. Y. Lee
48. D. K. Little
49. A. P. Malinauskas
50. A. J. Mattus
51. B. C. McCelland
52. Janis G. Pruett
53. D. E. Reichle
54. S. H. Stow
55. M. E. Timpson
56. J. R. Trabalka
57. J. H. Wilson
58. Central Research Library
59-73. ESD Library
74. ORNL Y-12 Technical Library
75-78. Laboratory Records Department
79. ORNL Patent Office

## External Distribution List

79. O. B. Adams, 6120 South Gilmore Road, Fairfield, OH 45014
80. R. B. Allen, DOE-FO, P. O. Box 398705, Cincinnati, OH 45239-8705
81. T. D. Anderson, U.S. Department of Energy, EM-551, 12800 Middlebrook Road, Germantown, MD 20874
82. J. A. Apps, Lawrence Berkeley Laboratory, University of California, Berkeley, CA 94720
83. L. Austin, Los Alamos National Laboratory, NMT-2, MS E501, P.O. Box 1663, Los Alamos, NM 87545
84. D. H. Bandy, TPO/AL, U.S. Department of Energy, P.O. Box 5400, Albuquerque, NM 87115
85. J. Berger, Office of Technology Integration, Westinghouse Hanford Co., P. O. Box 1970, MS LO-18, Richland, WA 99352
86. C. Bergren, Savannah River, Aiken, SC 29808
87. D. Berry, Department 6620, Sandia National Laboratory, Albuquerque, NM 87185-5800
88. J. Blakeslee, EG&G Rock Flats, Inc., Technology Development, P.O. Box 464, Golden, CO 80402-0464
89. M. Bollenbacher, IT Corporation, 312 Directors Drive, Knoxville, TN 37923
90. Art Bomberger, FERMCO, P. O. Box 398704, Cincinnati, OH 45239-8704
91. J. R. Brainard, LANL-INC-4, MS C346, Los Alamos National Laboratory, Los Alamos, NM 87545
92. D. J. Brettschneider, FERMCO, P. O. Box 398704, Cincinnati, OH 45239-8704
93. R. Brodzinski, PNL, Battelle Boulevard, Richland, WA 99352

94. D. J. Carr, FERMCO, P. O. Box 398704, Cincinnati, OH 45239-8704
95. R. Carrington, Plans & Programs Division, MSE Inc., P.O. Box 3767, CDIF, Butte, MT 59702
96. D. J. Chaiko, Argonne National Laboratory, Chemical Technology Division, 9700 South Cass Avenue, Argonne, IL 60439-4837
97. T. R. Clark, FERMCO, P. O. Box 398704, Cincinnati, OH 45239-8704
98. P. Colombo, Brookhaven National Laboratory, Building 703-50 Rutherford, Upton, NY 11973
99. L. A. Corathers, Battelle PNC, P. O. Box 999, Richland, WA 99352
100. J. Corones, AMES Laboratory, 329 Wilhelm Hall, Iowa State University, Ames, IA 50011
101. J. R. Craig, U.S. Department of Energy-FO, P. O. Box 398705, Cincinnati, OH 45239-8705
102. J. C. Cunnane, Argonne National Laboratory, 9700 South Cass Avenue, Argonne, IL 60439
103. H. Dugger, Daiser Engineers Hanford Co., Environmental Support Organization, P.O. Box 888, Richland, WA 99352
104. L. Dworjahyn, Westinghouse SRL, Building 779-2A, Aiken, SC 29808
105. D. A. Dzombak, Assistant Professor, Environmental Engineering, Department of Civil Engineering, Carnegie Mellon University, Pittsburgh, PA 15213-3890
106. L. Ebeling, REECO, P. O. Box 98521, Las Vegas, NV 89193
107. M. Elliot, EG&G Idaho, Inc., P. O. Box 1625, Idaho Falls, ID 83415-3420
108. D. Emilia, Strategic Planning Department, Chem-Nuclear Geotech, P. O. Box 14000, Grand Junction, CO 81502-2567
109. R. B. Evans, Ph.D., Environmental & Health Division, Reynolds Electrical & Engineering Co., P. O. Box 98521, Las Vegas, NV 89193-8521
110. L. S. England Farmer, FERMCO, P. O. Box 398704, Cincinnati, OH 45239-8704
111. R. N. Farvolden, Professor, Department of Earth Sciences, University of Waterloo, Waterloo, Ontario N2L 3G1 Canada
112. J. Fekete, P. E., Parsons, 6120 S. Gilmore Road, Fairfield Executive Center, Fairfield, OH 45014
113. C. J. Fermaintt, U.S. Department of Energy-FO, P. O. Box 398705, Cincinnati, OH 45239-8705
114. W. Fitch, U.S. Department of Energy, Idaho Field Office, 785 DOE Place, Idaho Falls, ID 83402
115. C. Frank, U.S. Department of Energy, EM-50, 6B-158/FORS, 1000 Independence Avenue, Washington, DC 20585
117. M. Fuhrmann, Brookhaven National Laboratory, Building 703M, Upton, NY 11973
118. A. Gatchett, RREL, 26 W. Martin Luther King Drive, Cincinnati, OH 45268
119. Richard Gay, Rockwell International, 6633 Canoga Avenue, Canoga Park, CA 91303
120. Doug Gerrick, FERMCO, P. O. Box 398704, Cincinnati, OH 45239-8704
121. V. Gil, FERMCO, P. O. Box 398704, Cincinnati, OH 45239-8704
122. R. Gilchrist, Technology Demonstration Programs, Westinghouse Hanford Co., P. O. Box 1970, MS L5-63, Richland, WA 99352
123. Rod Gimpel, FERMCO, P. O. Box 398704, Cincinnati, OH 45239-8704

124. R. L. Glenn, Parsons, 6120 South Gilmore Road, Fairfield, OH 45014
125. J. Gnosse, FERMCO, P. O. Box 398704, Cincinnati, OH 45239-8704
126. M. Gross, FERMCO, P. O. Box 398704, Cincinnati, OH 45239-8704
127. Bimleshwar Gupta, Solar Thermal Electric Program, Solar Energy Research Inst., 1617 Cole Boulevard, Golden, CO 80401
128. K. Hain, U.S. Department of Energy, EM-55, 12800 Middlebrook Road, Germantown, MD 20874
129. J. Hall, U.S. Department of Energy, Nevada Field Office, P. O. Box 998518, Las Vegas, NV 89193-8518
130. R. C. Harriss, Institute for the Study of Earth, Oceans, and Space, Science and Engineering Research Building, University of New Hampshire, Durham, NH 03824
131. B. F. Harvey, 6120 South Gilmore Road, Fairfield, OH 45014
132. J. Haugen, U.S. Department of Energy, Chicago Field Office, 9800 South Cass Avenue, Argonne, IL 60439
133. K. Hayes, U.S. Department of Energy, EM424, 12800 Middlebrook Road, Germantown, MD 20874
134. M. A. Heiskell, DOE/ORD, Waste Management Division (EW92), 200 Administration Road, Oak Ridge, TN 37831-8620
135. J. E. Helt, Ph.D., Director, Office of Waste Management Programs, 9700 South Cass Avenue, Argonne, IL 60439-4837
136. J. M. Hennig, U.S. Department of Energy, Richland Field Office, 825 Jadwin Avenue, P. O. Box 550, MS A5-21, Richland, WA 99352
137. D. Herman, FERMCO, P. O. Box 398704, Cincinnati, OH 45239-8704
138. William Holman, U.S. Department of Energy, San Francisco Field Office, 1333 Broadway, Oakland, CA 94612
140. J. Hyde, U.S. Department of Energy, EM-55, 12800 Middlebrook Road, Germantown, MD 20874
141. D. Jacoboski, FERMCO, P. O. Box 398704, Cincinnati, OH 45239-8704
142. R. Jacobson, Ph.D., University of Nevada, Water Resources Center, Suite 1, 2505 Chandler Avenue, Las Vegas, NV 89120
143. S. James, RREL, 26 W. Martin Luther King Drive, Cincinnati, OH 45268
144. R. J. Janke, U.S. Department of Energy-FO, P. O. Box 398705, Cincinnati, OH 45239-8705
145. G. Y. Jordy, Director, Office of Program Analysis, Office of Energy Research, ER-30, G-226, U.S. Department of Energy, Washington, DC 20545
146. P. G. Kaplan, Division 6312, Sandia National Laboratory, Albuquerque, NM 87185
147. T. R. Kato, FERMCO, P. O. Box 398704, Cincinnati, OH 45239-8704
148. K. Koller, EG&G Idaho, Inc., P. O. Box 1625, Idaho Falls, ID 83402-3970
149. Mike Krstich, FERMCO, P. O. Box 398704, Cincinnati, OH 45239-8704
150. D. Layton, Lawrence Livermore National Laboratory, P. O. Box 5507 (L-453), Livermore, CA 94550
151. D. Maiers, EG&G Idaho, Inc., Technology Development Dept., P. O. Box 1625, Idaho Falls, ID 83415-3940
152. M. Malone, U.S. Department of Energy, EM-551, Trevion II Bldg., Washington, DC 205850002

153. L. W. McClure, Westinghouse Idaho Nuclear Company, Inc., P. O. Box 4000, Idaho Falls, ID 83403-4000
154. T. McEvilly, 50E-111, Lawrence Berkeley Laboratory, 1 Cyclotron Road, Berkeley, CA 94720
155. K. Merrill (Acting), EG&G Idaho, Inc., P. O. Box 1625, Idaho Falls, ID 83415-3970
156. E. Merz, Waste Policy Institute, 12850 Middlebrook Road, Germantown, MD 20874
157. J. Mohiuddin, BDM Int., 12850 Middlebrook Road, Germantown, MD 20874
158. J. O. Moore, U.S. Department of Energy Oak Ridge Field Office, P. O. Box E, Oak Ridge, TN 37831
159. David Morris, INC-11 Actinide Team, MS C345, Los Alamos National Laboratory, Los Alamos, NM, 87545
160. H. D. Murphy, ET-AET, Los Alamos National Laboratory, MS D446, Los Alamos, NM 87545
161. M. Nickelson, HAZWRAP, P. O. Box 2003, Oak Ridge, TN 37831-7606
162. T. Noble, Center for Advanced Technology Development, Iowa State University, Ames, IA 50011

163-165. Kim Nuhfer, FERMCO, P. O. Box 398704, Cincinnati, OH 45239-8704

166. Lorie Oakes, HAZWRAP, P.O. Box 2003, Oak Ridge, TN 37831-7606
167. R. Olexsey, RREL, 26 Martin Luther King Dr., Cincinnati, OH 45268
168. R. H. Olson, Professor, Microbiology and Immunology Department, University of Michigan, Medical Sciences II, #5605, 1301 East Catherine Street, Ann Arbor, MI 48109-0620
169. M. O'Rear, U.S. Department of Energy, Savannah River Field Office, RFD #1, Building 703A, Room E208 North, P. O. Box A, Aiken, SC 29802
170. A. Patrinos, Director, Environmental Sciences Division, Office of Health and Environmental Research, ER-74, U.S. Department of Energy, Washington, DC 20585
171. R. W. Perkins, PNL, Battelle Boulevard, Richland, WA 99352
172. D. L. Perry, Lawrence Berkeley Laboratory, University of California, Berkeley, CA 94720
173. M. Peterson, Battelle Pacific NW Laboratory, P. O. Box 999, MSINP741, Richland, WA 99352
174. F. Poucher, Energy Programs & Advanced Planning, P. O. Box 1449-D/6222, T038, 6633 Canoga Avenue, Canoga Park, CA 91304
175. L. Rogers, EG&G/EM, P. O. Box 1812, Las Vegas, NV 89125
176. R. R. Ryan, T130-A, LATO, EG&G Rocky Flats, Golden, CO 80401
177. J. Sattler, FERMCO, P. O. Box 398704, Cincinnati, OH 45239-8704
178. P. A. Saxman, TPO/AL, U.S. Department of Energy, P. O. Box 5400, Albuquerque, NM 87115
179. A. Schilk, PNL, Nuclear Chemistry Department, Battelle Boulevard, Richland, WA 99352
180. J. Schnoor, 1134 Engineering Building, University of Iowa, Iowa City, IA 52242
181. Jim Schwing, FERMCO, P. O. Box 398704, Cincinnati, OH 45239-8704
182. R. S. Shirley, FERMCO, P. O. Box 398704, Cincinnati, OH 45239-8704
183. S. C. Slate, Pacific Northwest Laboratory, MSIN KI-25, Office of Environmental Tech., P. O. Box 999, Richland, WA 99352
184. R. Snipes, Martin Marietta-HAZWRAP, P. O. Box 2003, Oak Ridge, TN 37831-7606

185. S. Spence, Kaiser Engineering, MS E6-22, P. O. Box 888, Richland, WA 99352
186. Roger Stead, FERMCO, P. O. Box 398704, Cincinnati, OH 45239-8704
187. Larry Stebbins, FERMCO, P. O. Box 398704, Cincinnati, OH 45239-8704
188. J. L. Steele, P.E., Waste Environmental Remediation Programs, Savannah River Site, SRL, 733A, A208, Aiken, SC 29802
189. S. Stein, Deputy General Manager, Environmental Management Organization, Pacific Northwest Division, 4000 N.E. 41st Street, Seattle, WA 98105
190. K. Stevenson, U.S. Department of Energy, 376 Hudson Street, New York, NY 10014-3621
191. R. S. Stiger, Waste Technology Development, EG&G Idaho, Inc., P. O. Box 1625, Idaho Falls, ID 83415-3940
192. J. R. Suitlas, P. E., Senior Program Manager, Environmental Technologies Group, Halliburton Environmental Corporation, 661 Andersen Drive, Pittsburgh, PA 15220
193. T. M. Sullivan, Brookhaven National Laboratory, Building 830, Upton, NY 11973
194. R. E. Swatzell, HAZWRAP, P. O. Box 2003, Oak Ridge, TN 37831-7606
195. V. C. Tidwell, MS 6315, P. O. Box 5800, Sandia National Laboratory, Albuquerque, NM 87185
196. A. E. Torma, EG&G Idaho, P. O. Box 1625, Idaho Falls, ID 83415-3940
197. J. Walker, U.S. Department of Energy, Trevion II Bldg, Room 408, 12800 Middlebrook Road, Germantown, MD 20874.
198. F. J. Wobber, Environmental Sciences Division, Office of Health and Environmental Research, ER-74, U.S. Department of Energy, Washington, DC 20585
199. D. A. York, MEE-4, MS G787, P. O. Box 1663, Los Alamos National Laboratory, Los Alamos, NM, 87545
200. Office of Assistant Manager for Energy Research and Development, U.S. Department of Energy Oak Ridge Operations Office, P.O. Box 2001, Oak Ridge, TN 37831-8600

201-202. Office of Scientific and Technical Information, P. O. Box 62, Oak Ridge, TN 37831